



Low-pressure gasoline direct injection system development and emissions analysis for a reciprocating two-stroke engine

E. Gutiérrez¹ · D. Sala¹ · J. Delpéuch¹

Received: 15 May 2023 / Accepted: 23 March 2024 / Published online: 25 April 2024
© The Author(s) 2024

Abstract

This study presents the design and construction of an electronic low-pressure gasoline direct injection system for two-stroke engines, with the objective to study engine performance and the emission of exhaust polluting gases, maintaining the expectations of this type of engine. The investigation includes a test bench with an incorporated engine and the required control devices for this, as well as a gas analyzer Class 0, a computerized data acquisition and several tools for displaying and process all the electronic signals from the engine in real time. In order to manage this system, a custom electronic injection control unit has been designed and built, which allows to control the fuel injection timing and duration. This unit uses the signal from an inductive sensor installed in the crankshaft as a reference and synchronization point. Additionally, modifications have been made to the fuel feeder circuit and the electronic of the test engine, as well as to some parts of the mechanism in order to adapt them to this technology. The implementation of the engine tests is described, and the performance and operational points of the original system and those of the new injection system are evaluated.

Keywords Electronic fuel injection · Gasoline direct injection · Two-stroke engines

1 Introduction

The motorcycle industry has usually used carburetors or port fuel injection to fuel its two-stroke and four-stroke engines. In a carburetor-fed two-stroke engine, during the intake process (by valve or not) the carbureted air–fuel mixture is compressed into the crankcase below the piston and then fed into the cylinder via intake transfer. The main drawback with this fuel supply system is the fresh air–fuel mixture short-circuiting to the exhaust port during the scavenging process; this effect characterizes the fresh mixture leaving with the exhaust gas, thereby increasing fuel consumption and pollutant emissions, mainly unburned HC.

The implementation of port fuel injection to a two-stroke engine, with respect to carburetor fueling, produces an improvement in the combustion process, enhancements

in fuel economy and emissions can be achieved with this method. Nevertheless, once a two-stroke engine is equipped with direct fuel injection the combustion process changes completely, and the fuel short-circuiting can be almost minimized [1, 2].

Even though electric motorcycles are considered as a new trend of research and development, the existing internal combustion engines are one of the most widely power sources used under present-day circumstances.

There are several published studies on the operation of direct injection in two-stroke gasoline engines, and this work focuses on the development of a customized system using components available in any electronic fuel injection laboratory.

This study aims on the design and construction of a low-pressure gasoline direct injection system for two-stroke engines, as well as everything necessary for its control, including fuel feeding and processing of the reference signals.

This system, contrariwise to the high-pressure system, keeps the simplicity, the low weight and costs that are distinctive features essential for small two-stroke engines.

It is a good solution to implement a system that injects only fuel into the combustion chamber of the engine [3,

Technical Editor: Mario Eduardo Santos Martins.

✉ E. Gutiérrez
eegutierrez@mmt.upc.es

¹ Thermal Machines Laboratory, Higher Technical School of Industrial Engineers. Polytechnic University of Catalonia, Barcelona, Spain

4], unlike other systems that mix gasoline with previously compressed air [5–7], with good results, but significantly increase the cost and complexity of the entire installation.

Further, direct injection system can produce a stratified charge directly inside the combustion chamber with high evaporation rates, which limits fuel impingement on the cylinder walls and thereby reduces unburnt hydrocarbon emissions and fuel consumption.

This research analyses the functioning of a gasoline direct injection system and its electronic management. At the same time, an efficient and feasible to manipulate control system which allows full control of the injection, has been developed for this management.

Once the tests had been developed, the results are discussed and the conclusions are shown.

2 Experimental setup

2.1 Direct injection system developed for a reciprocating two-stroke engine

Direct injection systems are used on two-stroke engines to significantly reduce the amount of unburned fuel ejected into the exhaust port during the scavenging process by injecting fuel independently only when the exhaust port is closed and scavenging only with air charge. If possible, fuel short-circuiting should be avoided during the fuel injection, to minimize the loss of unburnt HC through the exhaust port.

A good experimental study on low-pressure direct injection is shown in [8, 9].

This premise, however, depends on the load conditions and engine speed, so it cannot always be achieved, mainly due to the temperature dependent propagation (sound speed) of the backloading scavenging wave from the exhaust.

Direct injection allows the implementation of a stratified combustion strategy, which the injection of very tiny fuel particles to allow fast fuel mixture formation for combustion. The achievement of this fuel spray preparation (vaporization) is very important in the execution of a stratified combustion process. This has the potential to improve the fuel economy significantly, even if the injection occurs partially during the fuel short-circuiting period. Several studies [10–13] show the impact of stratified combustion on the reduction of pollutant emissions and the increase in combustion efficiency.

Recently, the Japanese car manufacturer, MAZDA, has presented and patented [14] a novel two-stroke direct injection engine for automotive use, demonstrating the importance and validity of these engines.

2.1.1 Crankshaft electronic synchronization system

Every injection system requires a means of synchronization between the system and the reciprocating movement of the engine. This system allows the fuel to be supplied at a precise angle of the engine cycle. Currently, electronic synchronization is the most widespread [15].

The synchronization signal comes from the crankshaft, through an inductive sensor, the model used is a Magneti–Marelli SEN 8K3, whose analog output signal is sent to the conditioning and processing circuit.

Once the position of the sensor and receiver has been achieved, a signal is obtained for each angle of the engine cycle synchronized to 45° after TDC (Top Dead Center). In this way, there remains sufficient angle of the engine cycle to carry out the injection at any desired operating point, losing only in the 45°, which is also invalid as it corresponds to the expansion displacement of the piston.

2.1.2 Electronic injection control

In order to control the fuel injector, a signal is required which activates at the moment of the desired start of the injection, and which has a duration corresponding to the time interval that allows the injector to inject the necessary fuel into the combustion chamber in each situation.

The electronics developed for this function use a single signal for the synchronization, which is that coming from the crankshaft inductive sensor, and which is used as relative position of the piston to the TDC; it also allows determining the engine speed. From this point on, the electronics are responsible for delaying the reference signal and creating, as of this delay, a pre-established duration. Previous works by one of the author show research on the entire injection strategy for internal combustion engines [16, 17].

2.1.3 Processing of the reference signal

The signal from the inductive sensor first passes through a filter, which eliminates undesired components, and is then sent to an inverse logic gate. This eliminates the negative component of the signal leaving it in a square wave. Moreover, when inverted, it is ready for the next stage, which is activated by the falling edge of the signal.

A square signal is obtained from the previous conditioning stage, compatible with TTL technology, already prepared for processing. This stage is responsible for delaying the signal and, once initiated, gives the desired activation time.

The principal circuit of this task is NE555. This is a dual precision timer with two independent timer-type circuits. The conditioned signal must be passed to each branch of this circuit. In this way, two independent outputs signals

are obtained, causing the end of the first output signal to coincide with the start of the injection (timer 2) and the end of the second output signal to coincide with the end of the injection (timer 1). In this way, and after a process using

logical electronics in which the second signal is subtracted from the first, the desired signal is then obtained. Figure 1 shows this process graphically.

The injection timing adjust is conducted through two potentiometers electronically linked to the NE556 that controls timer 1 and timer 2, respectively.

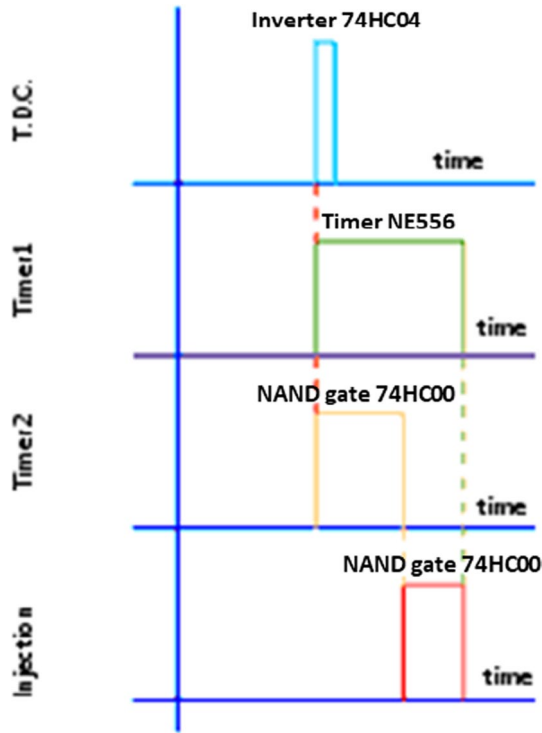


Fig. 1 Processing of the injection pulse signal

2.1.4 Injector controller

This electronic controller uses an injector drive controller (low impedance type) model LM1949. It consists of a peak and hold-type integrated circuit, which, properly mounted in a circuit (Fig. 2) including a Darlington transistor bridge, controls the intensity of the electric current passing through the injector. It supplies an initial peak intensity, guaranteeing the immediate opening of the injector, which is triple than of the following or holding stage, which must be just sufficient to keep the injector open.

Because it is a two-stroke engine, one injection is made at each crankshaft revolution, so the electronic implementation of a frequency divider for the injection is not necessary.

The Fig. 2 shows the complete electronic circuit diagram of the custom control unit developed for the fuel injection management. The two potentiometers in Fig. 2 control both the timing and duration of the fuel injection.

2.1.5 Fuel injector

The injector incorporated in the system is the HDEV 1.2 from the TFSI engines of the Volkswagen group, specifically

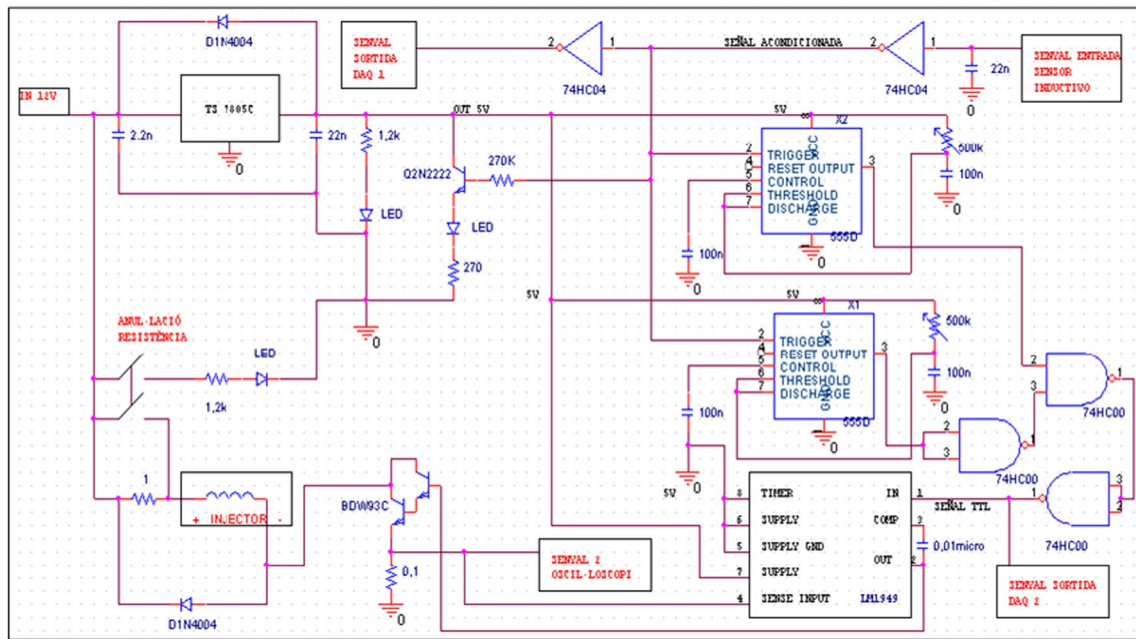


Fig. 2 Injection control system circuit diagram

the jets on two circles configuration, with the aim of decreasing the mean Sauter diameters of the spray droplets. This injector was chosen because it has to inject the fuel directly into the combustion chamber and therefore must withstand elevated temperatures and pressures.

The injector was calibrated in the laboratory to determine exactly the flow rate of injected fuel. For this purpose, 1000 injections were measured for different injection pulses, always at a constant injection pressure of 1 MPa. The resulting flow rate was 4.33 (mg/stroke)/msec.

From a geometrical point of view, the shape of this injector is appropriate for installation in the engine with the necessary modifications without affecting the mechanical strength of the cylinder head of the test engine.

2.2 Fuel feeder system

2.2.1 Cylinder head with built-in injector

The cylinder head was modified to place the fuel injector, resulting this way a direct injection system. To this end, a three-dimensional model in SolidWorks™ of the cylinder head was previously obtained, as it is shown in Fig. 3. With the assistance of this model, the injector was positioned to achieve good fuel vaporization and greatest cylinder fulfilling, in this work the optimal inclination angle of the injector was 50.91° with respect to the vertical plane.

The assembly of the injector on the cylinder head, mainly its inclination, is fitted considering the reduction of the fuel short-circuit, a good air–fuel homogenization and a minimal fuel impingement on the piston top. Very interesting studies about the importance of the position of the injector can be seen in [18–20].

The final installation of the injector in the cylinder head in the test engine is shown in Fig. 4. Due to the position of the injector, throughout the scavenge process, it is to be expected that the injected fuel is impregnated with the fresh

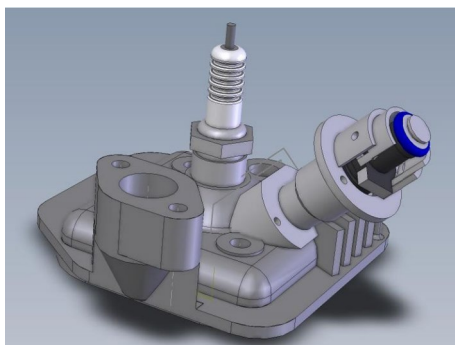


Fig. 3 Three-dimensional model of the installation of the fuel injector in the cylinder head

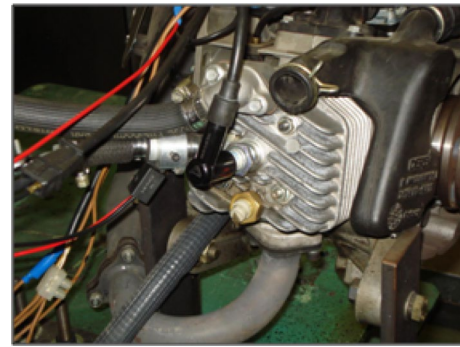


Fig. 4 Installation of the fuel injector in the cylinder head

air upcoming from the intake transfer and is directed toward the spark plug.

2.2.2 Fuel pump

The fuel requires an increment of pressure in order to be injected directly into the combustion chamber. One of the reasons is that in the engine cylinder the piston already provides pressure (compression phase), and in order to deliver the fuel, a higher pressure is necessary. The other reason is that the fuel must be introduced in the shortest period as possible, and it must be injected in an atomized form to facilitate a good mixture with air, mainly when the engine works with a homogeneous mixture for combustion [21]. That pressure is provided by the fuel pump, which, in this case, is a rotary pump from Volkswagen group, and the released fuel has a pressure greater than 1 MPa, so this pressure must be regulated subsequently.

2.2.3 Fuel pressure regulation

Whereas the test engine displacement is small (50 cm^3) and the compression pressure is relatively low, a higher injection pressure may be excessive, resulting in the injected fuel is impregnated into the piston head, affecting the process of mixture formation and therefore, combustion. Because of this, in the tests a relatively low injection pressure was used, however, the pressure regulator may be calibrated at a higher pressure according to the results of the tests in the engine or even future research.

In this work, a fuel pressure regulator at 1 MPa was used, which regulates the pressure through a membrane and a calibrated spring.

2.3 Electronic fuel injection management

2.3.1 Computer data acquisition system

When the injection tests are conducted from a reference point, it is very important to be aware of the current state

of the injector signal, when it is injecting, and the injection duration.

The importance of knowing and control when the gasoline is being injected is based on two facts. The first is that this is required in order to know at which point on the port timing of the engine the injection occurs (e.g., exhaust port open or closed). The second is to avoid injection when combustion is already occurring in the combustion chamber or during the expansion stroke, because of the risk this implies.

Two electronics signals are used for the analysis. The first is the inductive sensor signal and the second is that of the injector control device, which shows the intensity of the electric current of the injector divided by ten. By means of this system, the angles at which injector and ignition coil are activated, their duration, the time that remains from the end of the injection until ignition occurs and the rpm of the engine are graphically displayed.

In order to complete this type of monitoring, a data acquisition model, a PC and software that analyze and displays these data at the convenience of the researcher are all required.

2.3.2 Programming language

The programming language used was G. This is a powerful programming language as it represents the logic of the program through diagrams. This type of programming is known as visual programming, and in this study, the software LabVIEW™ was utilized. This is a graphic tool frequently used in engineering for data acquisition, instrument control and industrial automation.

2.3.3 Programming algorithm

The signals, obtained from the injector control device, are sent to the computer via digital counters, which are contained in their DAQ cards. These are introduced into the algorithm through the data acquisition function (DAQ Assistant).

To calculate the angular position of the start of the injection, the delay time between the sensor pulse and the start of the injection is measured and multiplied by the engine speed (in radians per second), thus obtaining the portion of the whole turning path. This portion of the path is converted into degrees and it is added to the 45° of the angular displacement existing between the sensor and TDC.

2.3.4 Front panel

The front panel is the interface with the researcher. This monitoring program communicate with the researcher so that the obtained results can be visualized always in real time.

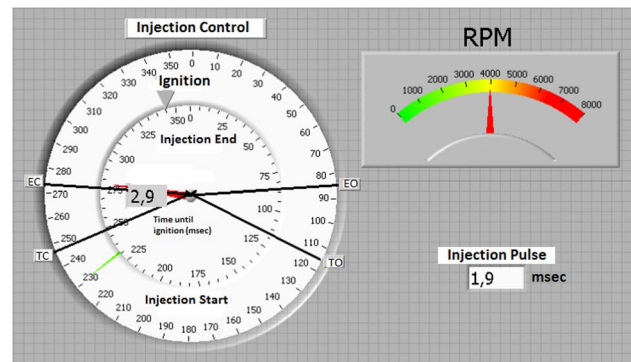


Fig. 5 Front panel of the computer monitoring

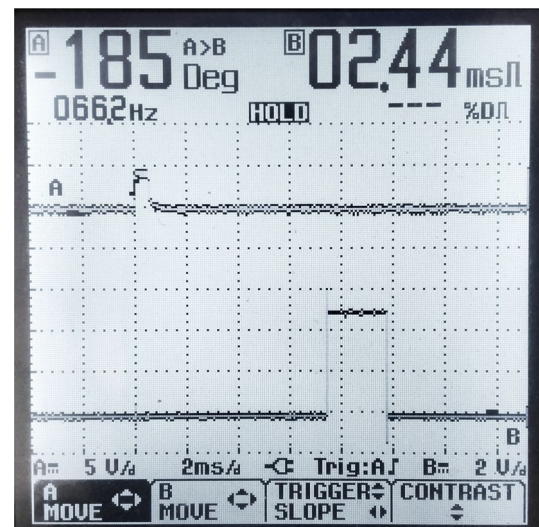


Fig. 6 Oscilloscope capture of the injector activation signal (channel B) and the reference signal from the engine crankshaft (channel A)

Figure 5 shows the front panel of the program used activated with the engine running at 4000 rpm (419 rad/s), an injection pulse of 1.9 ms, the start of the injection at 230° after TDC (green pointer), the end of the injection at 275.6° after TDC (red pointer) and a time until the spark ignition of 2.9 ms.

The Fig. 6 shows an oscilloscope capture of the injector activation signal (channel B) synchronized with the reference signal from the engine crankshaft (channel A) under similar conditions with Fig. 5.

A general diagram of the structure of systems including fuel delivery, electronic control of injection and the acquisition and monitoring signals is shown in Fig. 7.

2.3.5 Fuel injection strategy

The symmetrical scavenging port timings diagram of the test engine is shown in Fig. 8. To completely avoid

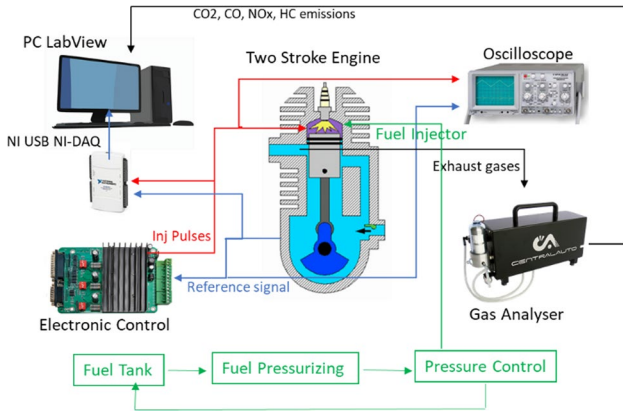


Fig. 7 General diagram of the system

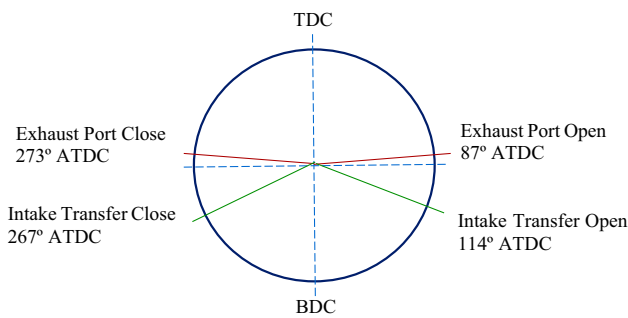


Fig. 8 Scavenging port timings diagram of the test engine

short-circuiting fuel to the exhaust, injection must be initiated at 273° ATDC, but as will be discussed below this is not always possible.

Figures 9, 10, 11 and 12 show the fuel injection timing during testing for different intake throttle openings. At low and medium engine speed, less than 4000 rpm (418 rad/s), further combustion stratification is desirable as possible, this is achieved by delaying the fuel injection as possible without affecting the combustion process [22–24].

With increasing speed and load, decreases the combustion stratification level by decreasing the injection timing [25], so combustion is performed with a homogeneous mixture. The charts show that it was not always possible to avoid fuel short-circuiting completely, mainly at high rpm with throttle opening of 60% and 90%, due to the short time period available for fuel injection. However, even for this condition, pollutant emissions were significantly lower, as will be seen in Results and discussion.

During the tests, numerous experimental analyses of the engine were carried out on the test bench, with the aim of adjusting the engine mapping considering mainly performance and emissions.

The mapping procedure aims to obtain the same or higher maximum performance of the base carbureted

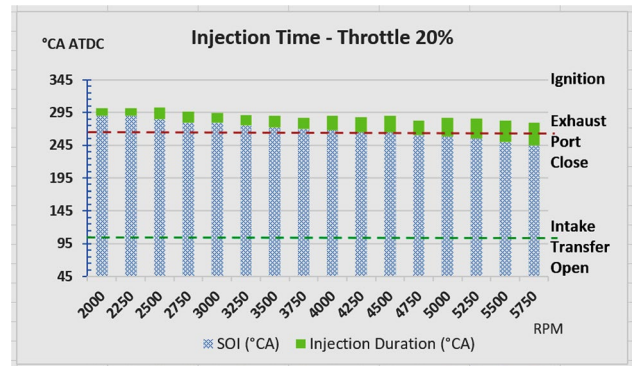


Fig. 9 Fuel injection timing for throttle opening 20%

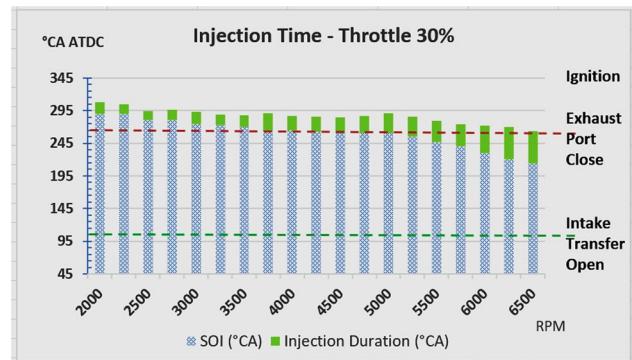


Fig. 10 Fuel injection timing for throttle opening 30%

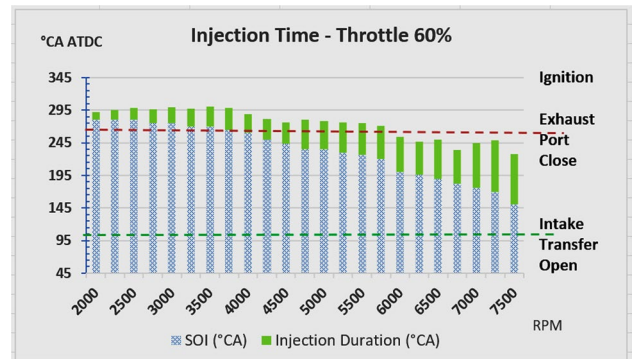


Fig. 11 Fuel injection timing for throttle opening 60%

engine with a great exhaust gas pollutant emissions reduction and improvement of efficiency in the whole working range, taking advantage of the accurate mapping of the fuel delivery (closer to the stoichiometric mixture).

The final injection map developed during the test is reported in Fig. 13.

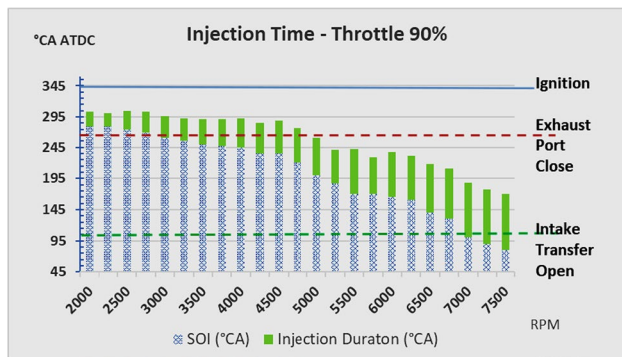


Fig. 12 Fuel injection timing for throttle opening 90%

3 Results and discussion

3.1 Study engine

To carry out the investigation, a Derbi Predator engine model was used and the parameters of which are specified in Table 1. The engine calibration and test were done at the test bench of the Laboratory of Thermal Machines of the Polytechnic University of Catalonia. The cell is provided with a Dynamic test bench APICOM model FR-30 with power 30 kW, nominal max torque 110 Nm and max speed 13,500 rpm. For the analysis of exhaust gases, an SPEKTRA model 3001 gas analyzer Class 0 was used, and a TECNER model 236C meter was used for the measurement of fuel consumption.

All tests were carried out under the same environmental conditions, and both the engine test bench and the measuring equipment were pre-calibrated by a specialized external company as part of a previous sponsored project by the Committee on Research Scientist of the Council of Government of the Polytechnic University of Catalonia.

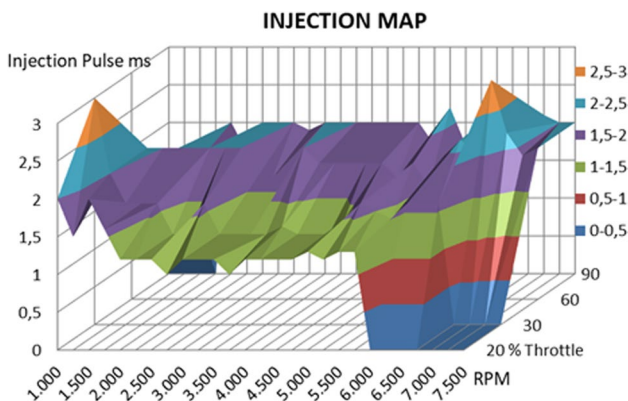


Fig. 13 Fuel injection mapping

Table 1 Test engine parameters

Engine	Two-stroke single-cylinder
Cooling	Water
Displacement	49 c.c
Compression	11:1
Port timing	Symmetrical, laminar
Fuel supply	Carburettor, Direct Injection
Ignition advance	18° B.T.D.C
Spark plug	NGK B9SE or Champion N2C
Fuel	98-Octane lead-free gasoline
Engine speed	7500 rpm max

The lubricating oil supply occurs separately from the fuel, to a specific reservoir. The supply of the lubricant to the engine takes place via a small rotary pump, which is powered by the engine crankshaft, making oil to mix with air in the crankcase, and flows into the cylinder through the intake transfer. The quantity of injected oil was adjusted in order to minimize the oil consumption and the pollutant emissions.

It should be noted that all tests and measurements were carried out without any post-combustion catalytic treatment of the exhaust gases.

3.1.1 Engine tests with carburetor

The obtained graph curves offer a great deal of information about the engine performance. As a reference when the characteristic graph curves of the engine running with injection are constructed, the graph curves obtained when the engine is operating with the carburetor are used.

In the graph of the Figs. 14 and 15, the trend of torque and power of the test engine can be seen for four different openings of the carburetor throttle, showing the typical reciprocating engine operation. As is known, the engine torque increase with the engine speed until a maximum value of torque is reached from which it begins to decrease.

In these tests with carburetor, the ignition timing remained constant with the original engine design, i.e., 18° B.T.D.C.

Due to the high engine speed, the volumetric efficiency becomes affected decreasing its value, in consequence, the combustion and total efficiency decrease. This combustion efficiency failure cannot be compensated for by an increase the amount of fuel injected, as discussed [26], and this is reflected in the maximums of the characteristic graph curves.

Figure 16 shows the air/fuel equivalence ratio of the mixture in the exhaust with the carburetor-fed engine. For throttle openings of 33% (with rpm above 4000), 60% and 85%, the composition of the air–fuel mixture is rich. This has a negative impact on both fuel consumption and the emission of polluting gases.

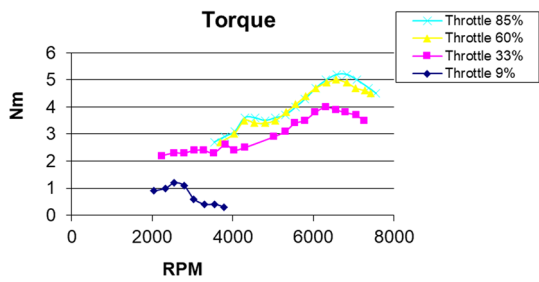


Fig. 14 Trend of torque vs. rpm of the engine with carburettor for different throttle openings

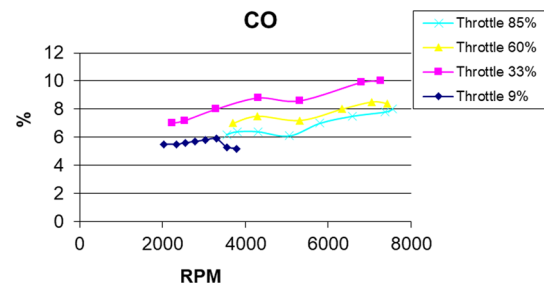


Fig. 17 CO emission vs. rpm of the engine with carburettor for different throttle openings

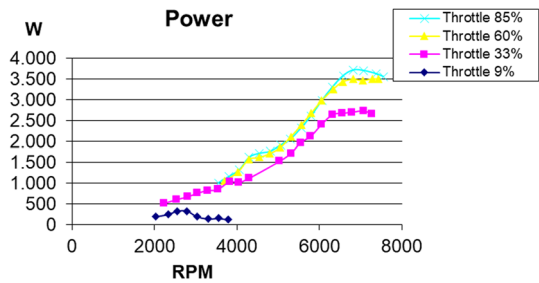


Fig. 15 Trend of power vs. rpm of the engine with carburettor for different throttle openings

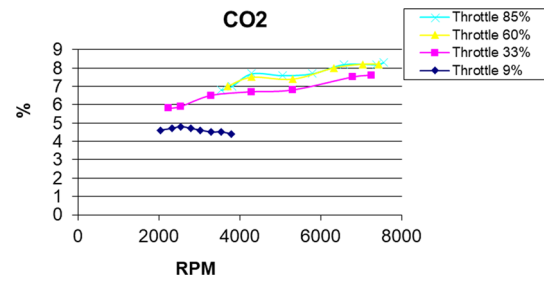


Fig. 18 CO₂ emission vs. rpm for the engine with carburettor for different throttle openings

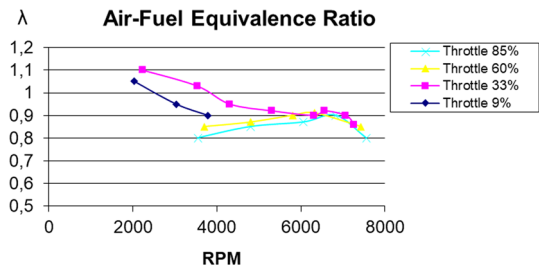


Fig. 16 Air–fuel equivalence ratio vs. rpm of the engine with carburettor for different throttle openings

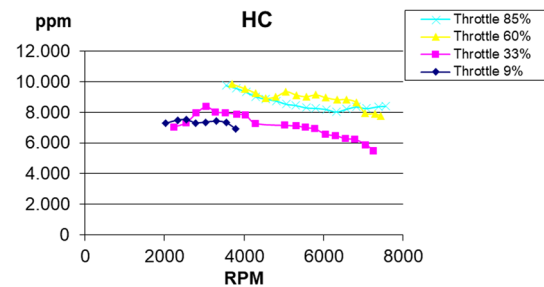


Fig. 19 HC emission vs. rpm of the engine with carburettor for different throttle openings

In the same way, the trend of CO and CO₂ emissions is reported in volume percentage of the exhaust gas in Figs. 17 and 18, respectively. Between the throttle openings of 60% and 85% CO₂ emissions are maximum, and the differences in the emission of CO₂ for these conditions are of little significance; this is because the throttle is practically fully open, so there is a too much presence of O₂, which logically favors the formation of CO₂ because much of the CO is oxidized forming CO₂. The difference is observed in the emission of CO for the different throttle openings in which, at a throttle opening of 85%, more O₂ enters the engine cylinder, decreasing the formation of CO during combustion. For a throttle opening of 9%, the fuel supply is minimal, so it is logical a minimum emission of all pollutants, except NO_x, due to a higher temperature in

the combustion chamber, as shown and explained later in Fig. 20.

The trend of HC and NO_x emissions is shown in ppm in Figs. 19 and 20, respectively. Obviously, the HC values are very high, mainly due to the working cycle of the test engine (two-stroke), as highlighted in the introduction of this work.

For medium and high loads, (throttle 60% and 85%) HC emissions are notably high; this is because the richness of the air–fuel mixture and the incomplete combustion from previous cycles aggravate the phenomenon of the fuel short-circuiting via the exhaust port during the scavenging process.

NO_x emission values are relatively low, mainly due to the low temperatures of the combustion process. This is

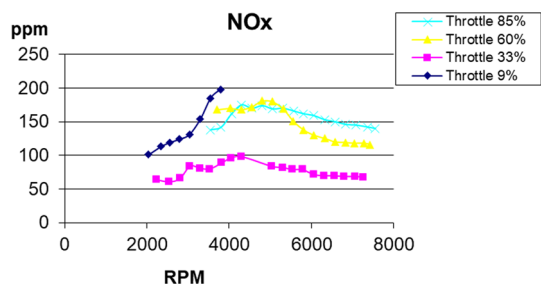


Fig. 20 NO_x emission vs. rpm of the engine with carburettor for different throttle openings

because the richness of the air–fuel mixture provided by the original carburetor of the base engine and the lubrication oil contribute to the cooling of the combustion chamber [27, 28]. For a throttle opening of 33%, there is a minimum of NO_x emissions, which coincides with a higher CO emission (Fig. 17), this is due to an excess of fuel in the mixture, which causes a greater cooling of the combustion chamber and, therefore, less emission of NO_x and higher CO emissions.

The specific fuel consumption of the engine is shown in Fig. 21. The best results were obtained for the 60% and 85% throttle openings, considerably higher than those achieved with direct injection for the same testing conditions, as shown and discussed later with respect to Fig. 30.

Knowing the BSFC and the lower heating value (LHV) of the European standard unleaded 98 gasoline (43.5 MJ/kg), the total efficiency was calculated according to Eq. (1).

$$\eta_t = \frac{1}{\text{BSFC} * \text{LHV}} \quad (1)$$

For carburetor testing, the total engine efficiency for different load and rpm conditions is shown in Fig. 22. These results are then analyzed in comparison with those obtained during direct injection tests.

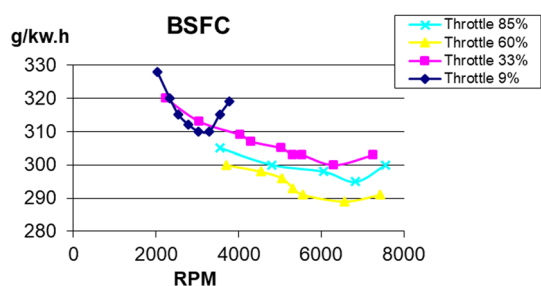


Fig. 21 Brake specific fuel consumption vs. rpm of the engine with carburettor for different throttle openings

3.2 Engine tests with electronic direct fuel injection

The tests with the engine functioning with direct fuel injection have been undertaken for four different openings of the intake throttle from those in the previous section, due to the different calibration of the control mechanism of the throttle aperture. The carburetor of the engine was kept up, to continue using the intake throttle, but its fuel supply was disabled. Despite this, the selected values are consistent with the previous ones.

For these tests, the ignition timing was set to minimum spark advance for maximum brake torque with knock-free combustion. After numerous tests, the ignition timing was adjusted at 15° B.T.D.C.

The entire electronic injection system, including fuel pump, is powered by the engine itself by means of a coupled alternator and battery, so this electrical power is subtracted from the power delivered by the test engine.

In order to obtain the graph curves, a frequency sweep was undertaken for each selected throttle opening. Initially, the aperture controller is positioned at the desired point and the test bench controller at 1000 rpm (105 rad/s). By means of the potentiometers of the electronic injector controller, the start and the duration of the injection for obtaining the maximum brake torque under knock-free conditions to these rpm are fixed. Then, the values of the torque, time from the start of the injection in milliseconds with respect to the signal of the inductive sensor, time of the duration of the injection in milliseconds and emissions in percentages respective to the volume of the emitted gas of CO and CO₂ are recorded, as well as HC and NO_x emissions in ppm. After this, the engine speed is increased by 250 rpm (26 rad/s) and the procedure is repeated successively until 7500 rpm (785 rad/s) is reached for each of the four openings of the intake throttle.

Although there are areas of operation of the engine where the torque delivered is greater, its operation is unstable, causing greater noise and vibrations, for this reason they have not been considered in this investigation. The main objective of this work is the operation close to the stoichiometric mixture for fuel economy, maintaining a

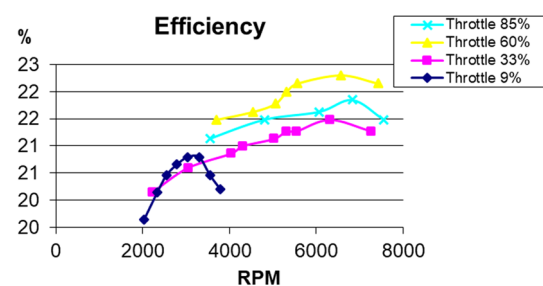


Fig. 22 Total efficiency vs. rpm of the engine with carburettor for different throttle openings

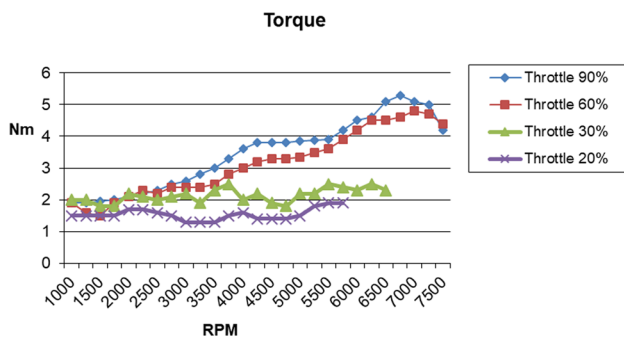


Fig. 23 Trend of torque vs. rpm of the engine running with direct fuel injection for different throttle openings

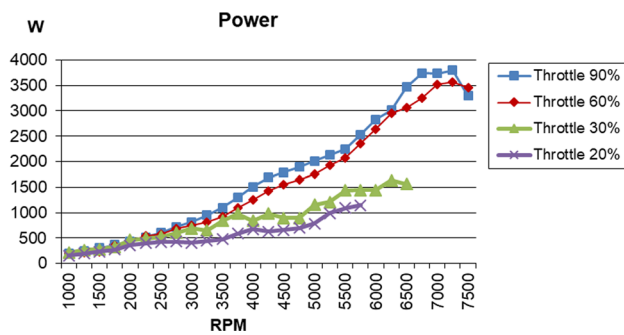


Fig. 24 Trend of power vs. rpm of the engine running with direct fuel injection for different throttle openings

stable operation of the engine. The results obtained can be observed in Figs. 23 and 24, showing the trend of torque and power of the test engine.

The engine performance with direct fuel injection can be seen again in the torque and power graph curves for four different openings of the intake throttle, marking a maximum and then they begin to decrease. This is because at high speeds the volumetric efficiency of the engine decreases (even with the intake throttle fully opened), which affects the combustion process, and therefore, the torque delivered.

Because the engine works with direct fuel injection, performance increases when the throttle aperture is greater [29], showing rising torque and power graph curves and high values for a 90% throttle aperture, it should be noted, as a positive factor, that for this condition the pumping losses during the scavenge process are lower. When the throttle aperture decreases, the values of torque and power also decrease until they produce unstable and irregular engine operation for throttle apertures of 30% and 20%.

In both cases, carburetion and direct injection, the performance of the engine is similar; however, they could be improved by increasing the amount of fuel injected, but as mentioned above, that is not the objective of this work.

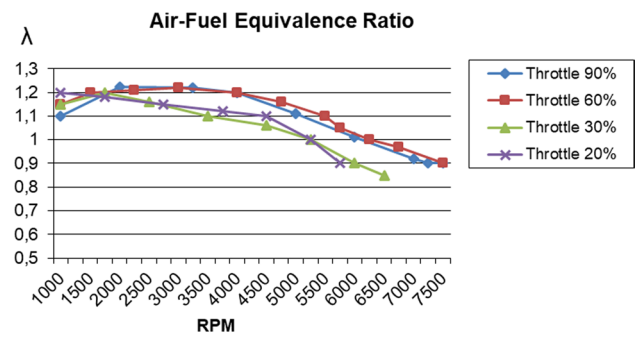


Fig. 25 Air fuel equivalence ratio vs. rpm of the engine running with direct fuel injection for different throttle openings

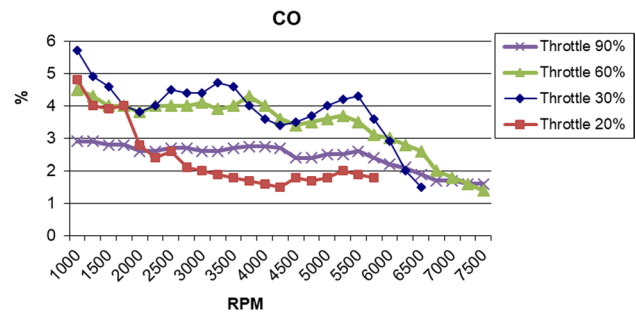


Fig. 26 CO emission vs. rpm of the engine working with direct fuel injection for different throttle openings

Figure 25 shows the air/fuel equivalence ratio of the mixture in the exhaust with the engine running on direct injection.

For these test conditions, after adjustment of the injection timing, stable engine operation was achieved with lean mixture up to 5000 rpm for all load conditions.

The graphics of the Figs. 26 and 27 shows the trend of CO and CO₂ emissions, respectively. The value of CO for the throttle opening of 90% is relatively low, and the CO₂ to the same conditions also, this is because small amount of fuel, in proportion to the quantity of the intake air, is injected, so the air–fuel mixture is too poor.

For low loads (throttle opening of 30%) and high rpm, the CO emissions are higher for both cases (carburetion and direct injection), even so, an average reduction of 53.8% is appreciated for the operation of the engine with direct fuel injection for this condition, and for a throttle opening of 60%, the average reduction was 55.9%. With the increase of the rpm, the CO emissions are significantly reduced, due to an increase in the efficiency of the combustion with direct fuel injection, and for full load (90% throttle opening), it is less than 3% in volume percentage of the exhaust gas for the whole engine speed range, well below 6.92% CO emissions on average with the engine working with carburetion for the same conditions.

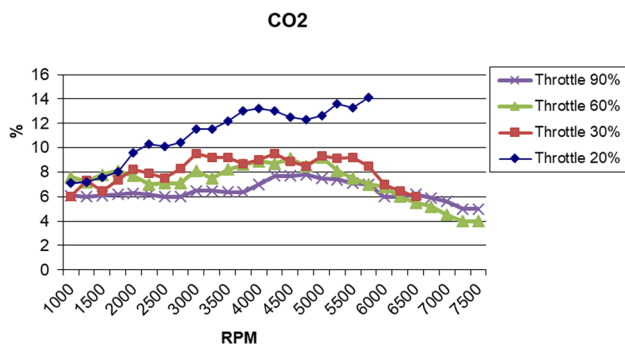


Fig. 27 CO₂ emission vs. rpm of the engine running with direct fuel injection for different throttle openings

CO₂ emissions decrease percentage-wise with the throttle aperture. For low loads (throttle opening of 30%), the average reduction is 17.8%, and for medium load (throttle opening of 60%), an average reduction of 6.5% has been achieved. For greater throttle aperture, the reduction is even bigger, and for a throttle opening of 90%, the CO₂ emission represented 6.42% on average of the exhaust gases, which represents an average decrease of 16.4% with respect to the operation of the engine with carburetion for these same conditions.

This CO₂ reduction with the increase of the throttle opening is mainly due to an increase in the efficiency of the combustion process.

HC and NO_x emissions are shown in Figs. 28 and 29, respectively. It should be noted that the emission of HC is higher for throttle opening of 60%, however, they are lower by 36.4% on average for the same conditions when the engine runs on carburetion, as shown previously in Fig. 18. For this condition, late injection decreases the HC exhaust port losses but negatively affects the air–fuel mixing process and conducts to unstable combustion because the time per stroke available for the injection is limited, and the amount of injected fuel per stroke is quite high, and on the contrary, too early start of the injection increases the

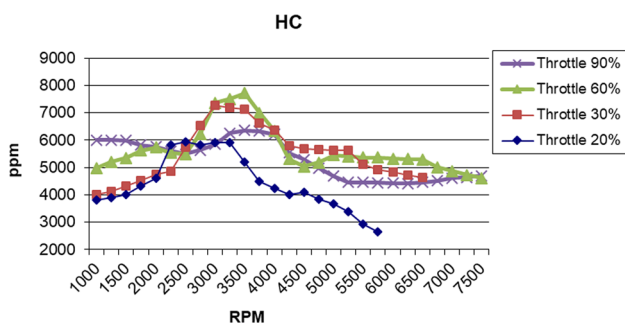


Fig. 28 HC emission vs. rpm of the engine working with direct fuel injection for different throttle openings

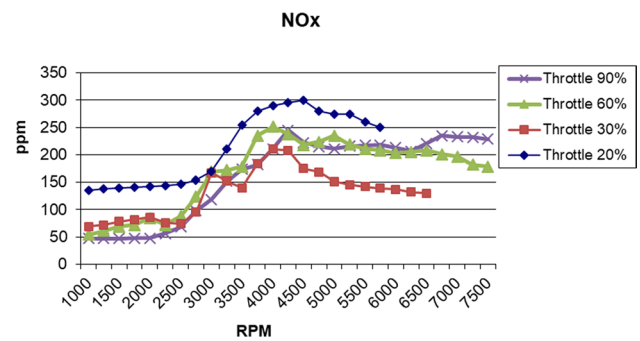


Fig. 29 NO_x emission vs. rpm of the engine running with direct fuel injection for different throttle openings

HC emission due the injected fuel is not engaged in the scavenge process and goes straight out through exhaust port, a specific study in this regard can be seen in [30]. Analyzing the full loads, being the most critical condition, the average reduction was 38.6%.

NO_x emissions are slightly higher for engine operation with direct fuel injection. For low loads (throttle opening of 20%), the increase is greater. It appears that the excessive strangulation of the intake airflow penalizes the scavenging process cycle by cycle, increasing the temperature of the combustion chamber and, therefore, the emission of NO_x. It is remarkable that these same conditions coincide with the lower emission of HC. For medium loads (60% throttle opening), the increase in NO_x emissions is about 15% on average, and for full load the average increase is only 3.8%. It should be noted that NO_x emissions could be effectively reduced by the control of the residual exhaust gas retained inside the cylinder (internal EGR) or the well-known external exhaust gas recirculation strategy.

The brake specific fuel consumption for the engine with direct fuel injection is shown in Fig. 30.

For low loads (throttle 20% and 30%), the BSFC is higher, but even under these conditions an average reduction of 8.5% and 9.7%, respectively, was achieved regarding the engine running on carburetor.

The BSFC is lower for a throttle opening of 60% and 90%, resulting in an average reduction of 13.6% and 9% compared to the same carburetor engine test conditions.

The total efficiency of the engine during direct injection testing is shown in Fig. 31.

For a throttle opening of 60%, the total efficiency is higher, achieving an average increase of 15.9% compared to the carburetor engine (shown in the Fig. 22). For the other load conditions, the improvement in total efficiency was smaller, but still significant: 10% for throttle opening of 90%, 10.9% for throttle opening of 30% and 9.2% for throttle opening of 20%.

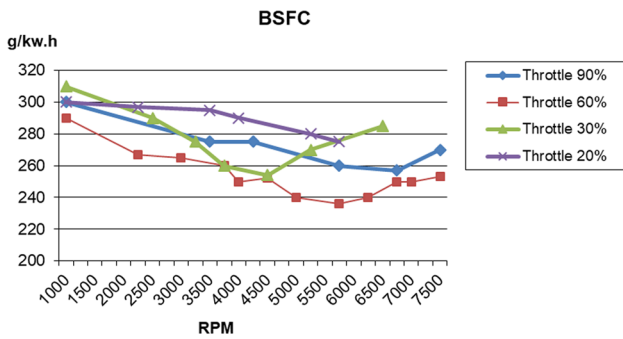


Fig. 30 Brake specific fuel consumption vs. rpm of the engine running with direct fuel injection for different throttle openings

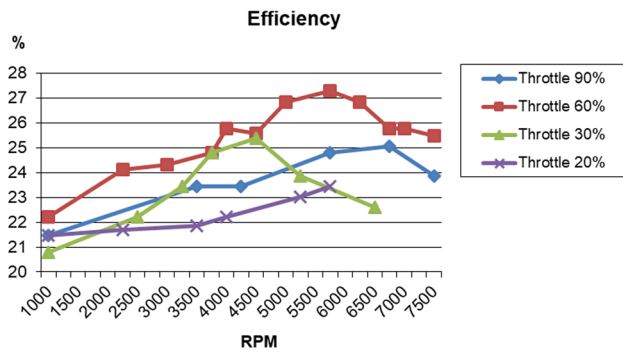


Fig. 31 Total efficiency vs. rpm of the engine working with direct fuel injection for different throttle openings

3.3 Uncertainty analysis

All measurements of physical magnitudes are subject to uncertainties. Uncertainty analysis was needed to prove the accuracy of the tests. The uncertainty in the computed values such as brake power measurements was estimated.

The measured values such as speed, voltage and current (from the electric brake of the test bench) and considering an efficiency (η_{ge}) of 0.85 were estimated from their respective uncertainties based on the Gaussian distribution. The uncertainties in the measured parameters are voltage (ΔV) \pm 3 V and current (ΔI) \pm 0.15A. For a speed (N) of 3500 rpm, voltage (V) of 220 V, current (I) of 13A and brake power (BP_w) of 3.4 kW, the uncertainty for brake power calculation is:

$$BP_w = f(V, I) = \frac{V * I}{\eta_{ge} * 1000} = 3.4 \text{ kW} \quad (2)$$

$$\frac{\delta BP_w}{\delta V} = \frac{3.4}{220} = 0.015$$

$$\frac{\delta BP_w}{\delta I} = \frac{3.4}{13} = 0.261$$

$$\Delta BP_w = \sqrt{\left(\frac{\delta BP_w}{\delta V} * \Delta V\right)^2 + \left(\frac{\delta BP_w}{\delta I} * \Delta I\right)^2} = 0.06 \text{ kW} \quad (3)$$

According to Eq. (3), the uncertainty in the brake power is \pm 0.06 kW and the uncertainty limits are 3.4 ± 0.06 kW.

Average uncertainties have been calculated considering the specifications of the measurement equipment offered by the manufacturers. The uncertainty estimation of all measured parameters is given in Table 2.

4 Conclusions

A low-pressure direct fuel injection system for two-stroke Otto cycle engines has been designed, implemented and valued. The results show a direct comparison of performance, fuel consumption and pollutants emissions of the same engine equipped with both a carburetor and direct injection system, for different load conditions and engine speed.

The main conclusion of this study is that the use of fuel-only low-pressure direct injection systems is feasible in two-stroke internal combustion engines, and its implementation is completely viable and it is not very expensive. The analyzed strategy is very hopeful; indeed, the modified engine achieves almost the same maximum performance as the base engine with an important increase in engine efficiency and significant reduction of HC emissions, that is, with the same engine performance, pollutant emissions can be decreased.

In this research, with the implementation of direct injection, stable engine operation was achieved with lean air–fuel mixtures (up to 1.2 air–fuel equivalence ratio), with the consequent reduction of fuel consumption. Overall engine efficiency was increased by 15.9% for half loads and approximately 10% for all other engine load conditions, which represents a very significant improvement.

Table 2 Accuracy and measurement uncertainty

Parameters	Unit	Uncertainty
Load	N	\pm 0.025 abs, \pm 0.5% rel
Speed	rpm	\pm 50 abs, \pm 1.0% rel
NO _x	ppm	\pm 20 ppm abs, \pm 4% rel
CO	%	\pm 0.02% abs, \pm 3% rel
HC	ppm	\pm 8 ppm abs, \pm 3% rel
CO ₂	%	\pm 0.03% abs, \pm 3% rel
Fuel	sec/100cm ³	\pm 0.1% abs, \pm 2% rel

The engine functioning with direct fuel injection could run with a maximum intake throttle aperture, in this way reducing the pumping losses during the intake process.

Considering pollutant emissions, the presented two-stroke direct fuel injection strategy can implement a pure oxidation catalyst.

During the engine operation at low and medium load and speed, it is possible to start the injection after closure of the exhaust port, avoiding fuel short-circuiting, in this way reducing the emission of unburnt HC and therefore decreasing the fuel consumption and the emission of contaminants.

This study shows the feasibility of the development of a system with relatively practical implementation into most of existing engines of this category, stimulating further investigation in this type of fuel injection management.

Acknowledgements This project was supported by the Committee on Research Scientist of the Council of Government of the Polytechnic University of Catalonia.

Funding Open Access funding provided thanks to the CRUE-CSIC agreement with Springer Nature.

Data availability All the necessary data to reproduce the results reported in Sect. 2.3 of this research are available from the corresponding author upon request.

Declarations

Conflicts of interests The authors declare that they have no competing financial interests or personal relationships that could have appeared to influence the work reported in this technical paper.

Open Access This article is licensed under a Creative Commons Attribution 4.0 International License, which permits use, sharing, adaptation, distribution and reproduction in any medium or format, as long as you give appropriate credit to the original author(s) and the source, provide a link to the Creative Commons licence, and indicate if changes were made. The images or other third party material in this article are included in the article's Creative Commons licence, unless indicated otherwise in a credit line to the material. If material is not included in the article's Creative Commons licence and your intended use is not permitted by statutory regulation or exceeds the permitted use, you will need to obtain permission directly from the copyright holder. To view a copy of this licence, visit <http://creativecommons.org/licenses/by/4.0/>.

References

- Pradeep V, Bakshi S, Ramesh A (2015) Direct injection of gaseous LPG in a two-stroke SI engine for improved performance. *Appl Therm Eng* 89:738–747. <https://doi.org/10.1016/j.applthermaleng.2015.06.049>
- Ferrara G, Balduzzi F, Vichi G (2012) An innovative solution for two-stroke engines to reduce the short-circuit effects. In: SAE Technical Papers. SAE International
- Leighton S, Ahern S (2003) Fuel economy advantages on Indian 2-stroke and 4-stroke motorcycles fitted with direct fuel injection. In: SAE Technical Papers. SAE International, pp 285–295
- Bertsch M, Beck KW, Matousek T, Spicher U (2013) Is a high pressure direct injection system a solution to reduce exhaust gas emissions in a small two-stroke engine?
- Boretti A, Jin S-H, Brear M et al (2008) Experimental and numerical study of a spark ignition engine with air-assisted direct injection. *Proc Inst Mech Eng Part D J Automob Eng* 222:1103–1119. <https://doi.org/10.1243/09544070JAUTO712>
- López JJ, Molina S, García A et al (2017) Analysis of the potential of a new automotive two-stroke gasoline engine able to operate in spark ignition and controlled autoignition combustion modes. *Appl Therm Eng* 126:834–847. <https://doi.org/10.1016/j.applthermaleng.2017.07.213>
- Chen Z, Liao B, Yu Y, Qin T (2022) Effect of equivalence ratio on spark ignition combustion of an air-assisted direct injection heavy-fuel two-stroke engine. *Fuel* 313:122646. <https://doi.org/10.1016/J.FUEL.2021.122646>
- Romani L, Vichi G, Balduzzi F et al (2017) Fine-tuning of a two stroke engine in full power configuration provided with a low pressure direct injection system. *Energy Procedia* 126:987–994. <https://doi.org/10.1016/j.egypro.2017.08.251>
- Loganathan M (2009) Ramesh A (2009) Experimental studies on low pressure semi-direct fuel injection in a two stroke spark ignition engine. *Int J Automot Technol* 10(10):151–160. <https://doi.org/10.1007/S12239-009-0018-0>
- Jung J, Park S, Bae C (2017) Combustion characteristics of gasoline and n-butane under lean stratified mixture conditions in a spray-guided direct injection spark ignition engine. *Fuel* 187:146–158. <https://doi.org/10.1016/J.FUEL.2016.08.085>
- He X, Zhou Y, Liu Z et al (2022) Impact of coolant temperature on the combustion characteristics and emissions of a stratified-charge direct-injection spark-ignition engine fueled with E30. *Fuel*. <https://doi.org/10.1016/J.FUEL.2021.121913>
- He X, Li Y, Sjöberg M et al (2019) Impact of coolant temperature on piston wall-wetting and smoke generation in a stratified-charge DISI engine operated on E30 fuel. *Proc Combust Inst* 37:4955–4963. <https://doi.org/10.1016/j.proci.2018.07.073>
- Shi L, Ji C, Wang S et al (2019) Impacts of dimethyl ether enrichment and various injection strategies on combustion and emissions of direct injection gasoline engines in the lean-burn condition. *Fuel* 254:115636. <https://doi.org/10.1016/J.FUEL.2019.115636>
- United States Patent Application: 0220034265 two-stroke engine with supercharger.
- Costa M, Sorge U, Merola S et al (2016) Split injection in a homogeneous stratified gasoline direct injection engine for high combustion efficiency and low pollutants emission. *Energy* 117:405–415. <https://doi.org/10.1016/j.energy.2016.03.065>
- Gutiérrez González E, Alvarez Flórez J, Arab S (2008) Development of the management strategies of the ECU for an internal combustion engine. *Mech Syst Signal Process* 22:1356–1373. <https://doi.org/10.1016/j.ymsp.2007.11.030>
- González EG, Flórez JA, Agramunt IC (2000) Improving the FIE mapping of a 4-cylinder 4-stroke engine for operation on the European drive cycle. In: SAE Technical Papers. SAE International
- Broatch A, Margot X, Novella R, Gomez-Soriano J (2017) Impact of the injector design on the combustion noise of gasoline partially premixed combustion in a 2-stroke engine. *Appl Therm Eng* 119:530–540. <https://doi.org/10.1016/J.APPLTHERMALENG.2017.03.081>
- Yang Y, Yu YS, Jeong M, Park S (2022) Mixture formation enhancement in a direct-injection spark-ignition engine using horizontal injection. *Fuel* 326:125121. <https://doi.org/10.1016/J.FUEL.2022.125121>
- Dalla Nora M, Diórdinis Metzka Lanzanova T, Eduardo Santos Martins M et al (2019) Experimental investigation of the air-fuel

- charging process in a four-valve supercharged two-stroke cycle GDI engine. *J Brazil Soc Mech Sci Eng* 41:132–133. <https://doi.org/10.1007/s40430-019-1638-6>
21. Johansen LCR, Hemdal S (2015) In cylinder visualization of stratified combustion of E85 and main sources of soot formation. *Fuel* 159:392–411. <https://doi.org/10.1016/j.fuel.2015.07.013>
 22. He BQ, Lin CL, Li X et al (2019) Numerical study of the mixture formation and stratified-flame-induced auto-ignition (SFI) combustion processes in a poppet-valve two-stroke direct injection gasoline engine. *Appl Therm Eng* 152:654–665. <https://doi.org/10.1016/J.APPLTHERMALENG.2019.02.025>
 23. Aljamali S, Abdullah S, Wan Mahmood WMF, Ali Y (2016) Effect of fuel injection timings on performance and emissions of stratified combustion CNGDI engine. *Appl Therm Eng* 109:619–629. <https://doi.org/10.1016/j.applthermaleng.2016.08.127>
 24. Ning L, Duan Q, Wei Y et al (2019) Effects of injection timing and compression ratio on the combustion performance and emissions of a two-stroke DISI engine fuelled with aviation kerosene. *Appl Therm Eng* 161:114124. <https://doi.org/10.1016/j.applthermaleng.2019.114124>
 25. Su Y-H, Kuo T-F (2019) CFD-assisted analysis of the characteristics of stratified-charge combustion inside a wall-guided gasoline direct injection engine. *Energy* 175:151–164. <https://doi.org/10.1016/j.energy.2019.03.031>
 26. Benajes J, Martín J, Novella R, Thein K (2016) Understanding the performance of the multiple injection gasoline partially premixed combustion concept implemented in a 2-Stroke high speed direct injection compression ignition engine. *Appl Energy* 161:465–475. <https://doi.org/10.1016/j.apenergy.2015.10.034>
 27. Merola SS, Irimescu A, Marchitto L et al (2017) Effect of injection timing on combustion and soot formation in a direct injection spark ignition engine fueled with butanol. *Int J Engine Res* 18:490–504. <https://doi.org/10.1177/1468087416671017>
 28. Ji W, Li A, Lu X et al (2019) Numerical study on NOx and ISFC co-optimization for a low-speed two-stroke engine via Miller cycle, EGR, intake air humidification, and injection strategy implementation. *Appl Therm Eng* 153:398–408. <https://doi.org/10.1016/j.applthermaleng.2019.03.035>
 29. Peng M, Deng X, Liang X (2011) Control strategy & calibration of fuel injection impulse width on EFI motorcycle engine. In: 2011 international conference on electric information and control engineering. IEEE, pp 2047–2053
 30. Lee Z, Kim T, Park S (2020) Influences of exhaust load and injection timing on particle number emissions in a gasoline direct injection engine. *Fuel* 268:117344. <https://doi.org/10.1016/J.FUEL.2020.117344>

Publisher's Note Springer Nature remains neutral with regard to jurisdictional claims in published maps and institutional affiliations.